

Y. Yi<sup>1</sup>, P. Minnis<sup>2</sup>, J. Huang<sup>1</sup>, J. K. Ayers<sup>1</sup>, D. R. Doelling<sup>1</sup>, M.M. Khaiyer<sup>1</sup>, M. L. Nordeen<sup>1</sup>

<sup>1</sup>Analytical Services & Materials Inc. VA 23666

<sup>2</sup>NASA Langley Research Center, Hampton, VA 23681

## 1. INTRODUCTION

Cloud parameterizations require basic knowledge of the relationships between measured and modeled meteorological state parameters and the cloud properties in a given volume of air. The uncertainty in the relationships, which is especially large for cirrus clouds, is exacerbated by the differences between actual soundings and those produced by various models. Routine surface cloud observations view only the lowermost cloud layers in a column while satellites see only the uppermost cloud layer. With the availability of high temporal resolution Active Remotely Sensed Cloud Location (ARSCL, Clothiaux et al. 2001), radiosondes, and satellite retrievals of cloud properties over the ARM (Atmospheric Radiation Measurement) Southern Great Plains central facility (SCF) site, it is possible to better quantify the relationship between meteorological state parameters and the cloud properties in a given volume of air. This study examines the relationships and differences between modeled and ARM-measured meteorological state parameters in clear and cloudy conditions and develops a temperature-dependent relative-humidity dependent cloud detection method. The resulting empirical models can be used to estimate the probability of cloud occurrence within a given atmospheric layer.

## 2. DATASETS

The modeled atmospheric profiles of height, temperature, RH, and horizontal and vertical wind speeds were derived from the 40-km resolution, 1-hourly Rapid Update Cycle (RUC40) analyses (Benjamin et al., 2004a and 2004b) in 25-hPa intervals from the surface to 100 hPa. The values at the RUC grid point closest to the SCF (36.617 °N, 97.5 °W) are used here.

Radiosonde (SONDE) data collected at the SCF from 1 March 2000 to 28 February 2001 were used as the best available atmospheric profiles. There are normally four radiosonde launches per day, at 00, 06, 12, and 18 UTC, respectively. During intensive observing periods, which typically occur 3–5 times per year, radiosondes are launched 8 times per day at the SCF. They provide high-resolution profiles of pressure, temperature, relative humidity with respect to liquid water, and wind speed and direction. The reported values cover the pressure range from the surface to maximum observation level.

To reduce RH measurement noise and facilitate processing, the radiosonde profiles were vertically smoothed into 25-hPa interval profile from the surface to 100 hPa. The time of the sounding midpoint was determined for each radiosonde ascent and matched with the closest hourly RUC analysis profile. The RH from both SONDE and RUC data is defined with respect to liquid water at all temperature and is converted to RH with respect to ice (RHI) at temperatures less than or equal to 253 K since most clouds are composed of ice when the temperature  $T < 253$  K. The ARSCL cloud product consists of cloud base and top heights determined for each 10-second interval using the algorithms of Clothiaux et al. (2001) with a combination of Belfort Laser Ceilometer (BLC), Millimeter Wave Cloud Radar (MMCR), and Micropulse Lidar (MPL) data. The cloud base and top heights used in this study are 10-min averages centered on the RUC times.

## 3. RESULTS

The combined dataset consists of 1150 soundings matched with RUC profiles and ARSCL cloud boundary data. From the ARSCL cloud boundaries, each layer in the SONDE and RUC data can be identified as being either a cloud-free or cloudy. If all layers are cloud-free for a given profile, then it is defined as a clear-sky sounding, otherwise, as a cloudy-sky sounding. About 60% of these soundings or RUC profiles are classified as clear-sky soundings with the remaining 40% classified as cloudy-sky soundings. Figure 1 shows scatter plots of the relative humidity and temperature from SONDE and RUC data in the upper troposphere (250 - 350 hPa) inside clouds. The temperature observations from the SONDE and RUC are highly correlated. The RHs are somewhat correlated, but the SONDE values are generally greater than those from RUC. These results were expected since comparisons of matched SONDE and RUC tend to show that the RUC RH is lower than its SONDE counterpart at higher values of RH. This bias may be due to the RUC model constraining humidity values. The radiosonde, being a point measurement, reports the actual instrument-measured atmospheric thermodynamic state if the biases in RH due to instrument errors (Wang et al., 2002; Turner et al., 2003) are ignored. Thus, the RUC may not reflect or capture some cloud information, especially for short term and small-scale cloud systems. For both datasets, the frequency distributions are distinctly different between clear and cloudy conditions for all layers. (Figures are not shown). The SONDE histograms are more peaked compared to the smoothed RUC data. The large fluctuations in RH result in a heavy-tailed frequency distribution. The ice-supersaturation layers exist both inside clouds and

outside clouds in the upper troposphere (100 hPa – 400 hPa).

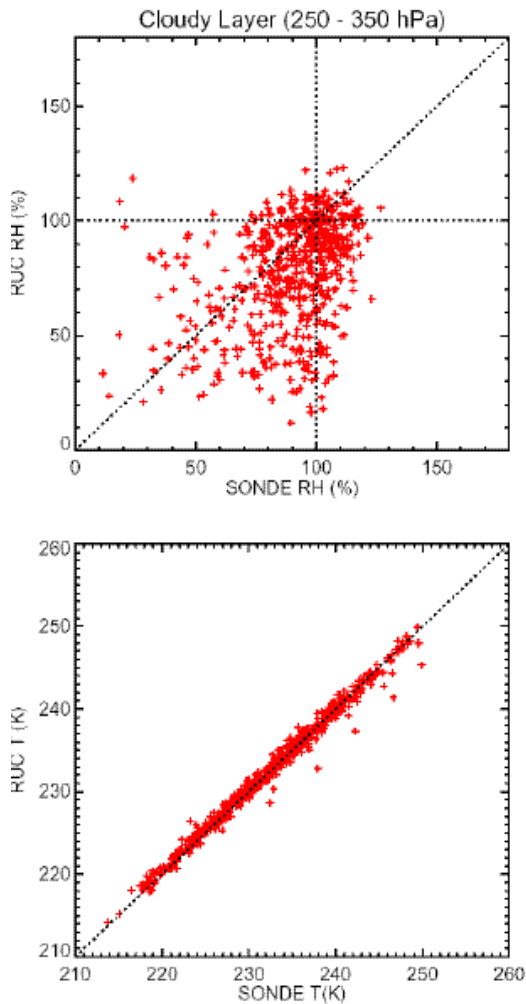


Fig. 1. Scatterplots of relative humidity and temperature inside clouds from SONDE and RUC, 250- 350 hPa.

The vertical distributions of RH and T difference between SONDE and RUC data in clear and cloud conditions are shown in Fig. 2. Inside clouds (blue curve), the RH from RUC is 2-14 % lower than the RH from SONDE for all RUC layers. There is no significant RH difference between SONDE and RUC data outside of clouds (red curve) or in clear sky (brown curve) in the lower troposphere (below 500 hPa). Above 500 hPa, however, the RUC seems to be moister than the SONDE with the difference between SONDE and RUC increasing with height (decreasing pressure), especially in the upper troposphere.

In order to find the relationships between RH cloud thresholds and temperature, the RH values are grouped according to the associated ambient temperature resulting in a frequency distribution for each temperature interval. Figure 3 shows the frequency distributions of RH when the ambient temperature is

between 250 and 254 K. The histogram (solid blue steps) and Gaussian fit (blue dotted line) are presented together in the upper panel. The cumulative distribution functions in clear and cloudy conditions are shown in

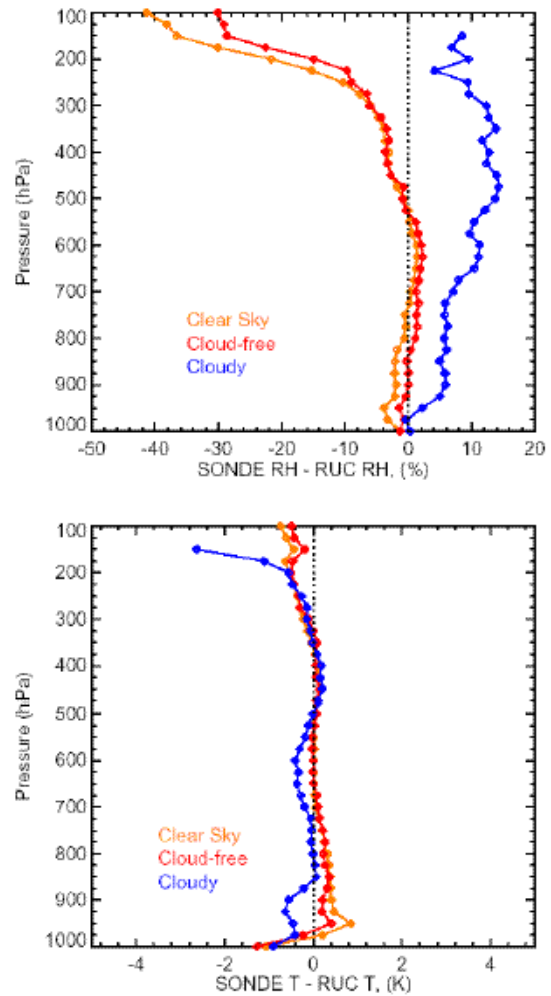


Fig. 2. Vertical distribution of RH and T differences between SONDE and RUC in clear and cloudy conditions.

the lower panel of Fig. 3. The blue solid and dotted lines show that the histogram and Gaussian fit are in good agreement, which indicates that the relative humidity inside clouds can be described by a Gaussian (normal) distribution. However, the relative humidity outside of clouds (red) and in the clear sky (brown) cannot be represented by a normal distribution but might fit better to an exponential distribution. Ovarlez et al. (2002) also found that the relative humidity statistics outside and inside of clouds are fundamentally different: the relative humidity within clouds turns out to be better described by either a Gaussian or a Rayleigh distribution centered at saturation. From the cumulative distribution functions (lower panels of Fig. 3), it can be seen that, when  $RH < 67.52\%$  for SONDE and  $RH < 48.37\%$  for RUC, the probability of finding a cloud is 20%. In other words, the

RH threshold value, with 20% probability of finding a cloud, is 67.52% for SONDE and 48.37% for RUC. Similarly, the RH thresholds can be determined at different probabilities (40%, 60%, and 80%) of finding a cloud.

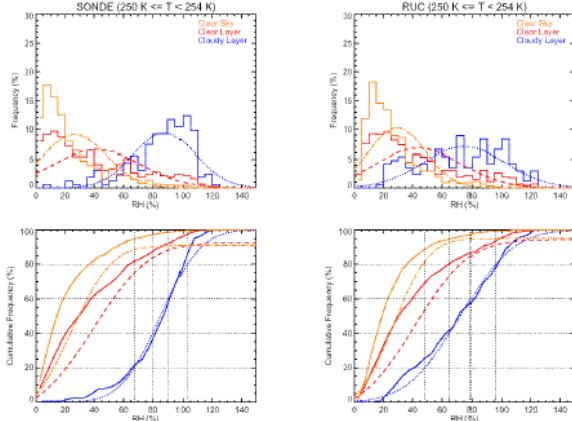


Fig. 3. Frequency distributions of RH from all cloud layers where the ambient temperature is greater than 250 K and less than 254 K, for both SONDE and RUC.

By repeating the above procedures for other RH groups and plotting RH frequency distributions versus temperature, the frequency of cloud occurrence for a given RH and T is easily determined. The two-dimensional frequency distributions of cloud occurrence for both SONDE and RUC data are shown in Fig. 4. The relative humidity threshold values used to make the cloud diagnoses with different probabilities for the RUC and SONDE are shown as red lines in Fig. 4. The drops in the thresholds around 255 K are due to the switch from RH with respect to water to RH<sub>i</sub>. When T is less than 245 K, the RH thresholds do not vary much with temperature. At the same probability, the RH thresholds for SONDE are higher than those for RUC except at warmer temperatures (T > 284 K).

Knowing the probability of finding a cloud at a given RH and T, then a sounding can be used to estimate the potential for cloudiness at a given level in the atmosphere. In other words, an atmospheric profile from RUC or SONDE can be used to construct a 3-D cloud dataset. In order to estimate the probability,  $P_{cloud}$ , of finding a cloud at a given RH and T, empirical models were developed from the RUC and SONDE data:

$$P_{cloud}(T, RH) = A_0 + A_1 e^{-\frac{[\zeta_1(T, RH) + \zeta_2(T, RH)]}{2}} \quad (1)$$

where

$$\zeta_1(T, RH) = \left\{ [(T - A_2) \sin A_4 + (RH - A_3) \cos A_4] / A_5 \right\}^2$$

$$\zeta_2(T, RH) = \left\{ [(T - A_2) \cos A_4 - (RH - A_3) \sin A_4] / A_6 \right\}^2$$

The coefficients  $A_i$  ( $i=0, 6$ ) have different values for the RUC and SONDE datasets and for warm ( $T > 254$ ) and cold ( $T < 254$ ) clouds. Figure 5 shows an example of the 3-D cloud distribution derived from Eq. (1) using RUC data. It demonstrates that this approach can be used to describe 3-D cloud structure.

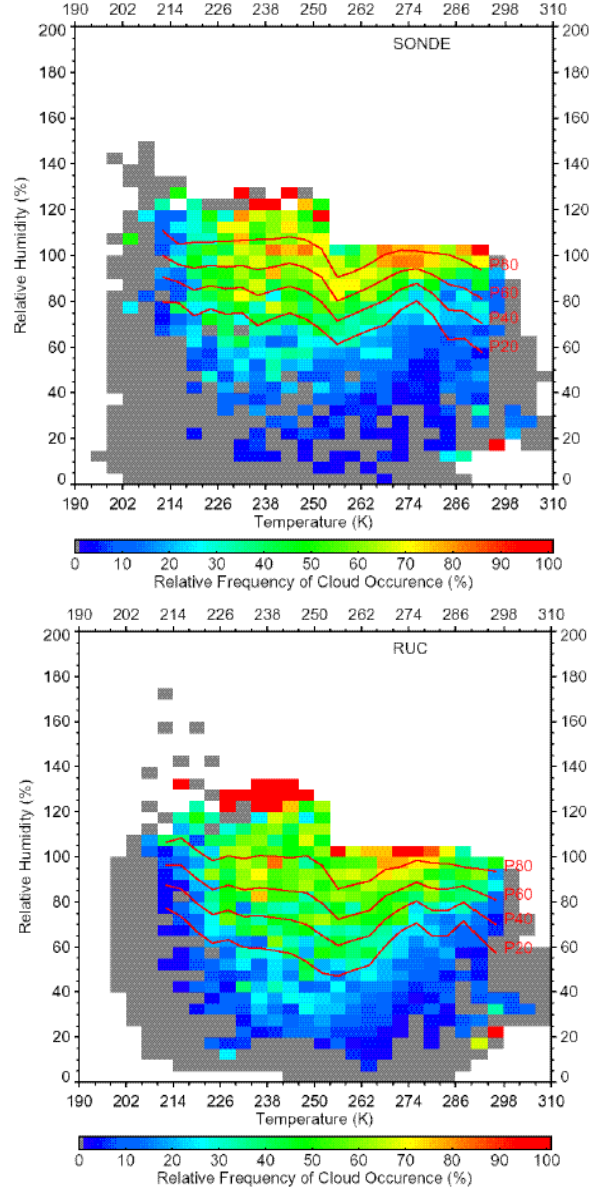


Fig. 4. Two-dimensional frequency distribution of cloud occurrence for a given RH and T for both SONDE and RUC data.

#### 4. SUMMARY

In this study, hourly RUC analyses were used to examine the differences between RH and temperature values from RUC reanalysis data and from radiosonde atmospheric profiles obtained at the ARM SCF. The results show that the temperature observations from the

SONDE and RUC are highly correlated. The RHs are also well-correlated, but the SONDE values generally exceed those from RUC. Inside cloud layers, the RH from RUC is 2-14 % lower than the RH from SONDE for all RUC layers. Although the layer mean RH within clouds is much greater than the layer mean RH outside cloud or in the clear-sky, RH thresholds chosen as a function of temperature can more accurately diagnose cloud occurrence for either dataset. For overcast clouds, it was found that the 50% probability RH threshold for diagnosing a cloud, within a given upper tropospheric layer is roughly 90% for the Vaisala RS80-15LH radiosonde and 80% for RUC data. While for the partial cloud (cloud amount is less than 90%), the RH thresholds of SONDE are close to RUC for a given probability in upper tropospheric layers. The probabilities of detecting clouds at a given RH and temperature should be useful for a variety of application such as the development of new cloud parameterizations or for estimating the vertical profile of cloudiness underneath a given cloud observed from the satellite to construct a 3-D cloud data set for computing atmospheric radiative heating profiles or determining potential aircraft icing conditions.

## 5. ACKNOWLEDGEMENTS

This research was supported by the Environmental Sciences Division of U.S. Department of Energy through the Interagency Agreements DE-AI02-97ER62341 and DE-AI02-02ER63319 under the ARM program and by the NASA Advanced Satellite Aviation Products project.

## 6. References

- Benjamin, S. G., G. A. Grell, J. M. Brown, T. G. Smirnova, and R. Bleck (2004a), Mesoscale weather prediction with the RUC hybrid isentropic/terrain-following coordinate model. *Mon. Wea. Rev.*, 132, 474-494.
- Benjamin, S. G., and Coauthors (2004b), An hourly assimilation/forecast cycle: The RUC. *Mon. Wea. Rev.*, 132, 495-518.
- Clothiaux, E.E., M.A. Miller, R.C. Perez, D.D. Turner, K.P. Moran, B.E. Martner, T.P. Ackerman, G.G. Mace, R.T. Marchand, K.B. Widener, D.J. Rodriguez, T. Uttal, J.H. Mather, C.J. Flynn, K.L. Gaustad, and B. Ermold (2001), The ARM Millimeter Wave Cloud Radars (MMCRs) and the Active Remote Sensing of Clouds (ARSCL) Value Added Product (VAP), DOE Tech. Memo. ARM VAP-002.1.
- Ovarlez, J., J.-F. Gayet, K. Gierens, J. Strom, H. Ovarlez, F. Auriol, R. Busen, and U. Schumann, (2002), Water vapor measurements inside cirrus clouds in northern and southern hemispheres during INCA. *Geophys. Res. Lett.*, 29, 1813.
- Turner, D., B. Lesht, A. Clough, J. Liljegren, H. Revercomb and D. Tobin (2003), Dry Bias and Variability in Vaisala RS80-H Radiosondes: The ARM Experience, *J. Atmos. Oceanic Technol.*, 20, 117-132.
- Wang, J., H. Cole, D. J. Carlson, E. R. Miller, K. Beierle, A. Paukkunen, and T. K. Laine (2002), Corrections of humidity measurement errors from the Vaisala RS80 radiosonde Application to TOGA/COARE data. *J. Atmos. Oceanic Technol.*, 19, 981- 1002.

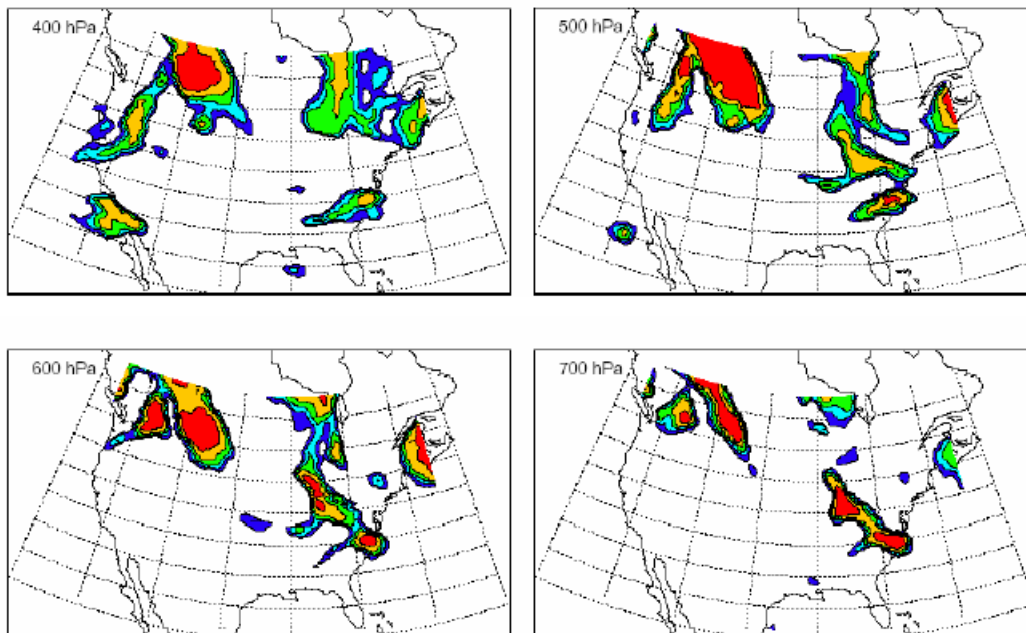


Figure 5. Distribution of cloud probability at 400 hPa, 500 hPa, 600 hPa and 700 hPa for 1900 UTC, 18 March 2004 over continental US. The red color is for probability greater than 90%, orange for 80% -90%, green for 70%-80%, light blue for 60%-70% and blue for 50%-60%.